Geochemistry Geophysics Geosystems G3
AN ELECTRONIC JOURNAL OF THE EARTH SCIENCES
Published by AGU and the Geochemical Society

Article
Volume 3, Number 1
31 January 2002
10.1029/2001GC000178
ISSN: 1525-2027

Behavior of Li and its isotopes during serpentinization of oceanic peridotites

Sylvie Decitre
CRPG-CNRS, 15 rue Notre-Dame des Pauvres, 54501 Vandoeuvre les Nancy Cedex, France

Now at Département de Géosciences, Université de Franche-Comté, 16 Route de Gray 25030 Besançon Cedex, France (sylvie.decitre@univ-fcomte.fr)

Etienne Deloule and Laurie Reisberg
CRPG-CNRS, 15 rue Notre-Dame des Pauvres, 54501 Vandoeuvre les Nancy Cedex, France (deloule@crpg.cnrs-nancy.fr; reisberg@crpg.cnrs-nancy.fr)

Rachael James
Department of Earth Sciences, The Open University, Walton Hall, Milton Keynes, MK7 6AA, England (R.H.James@open.ac.uk)

Pierre Agrinier
Laboratoire de Geochimie des Isotopes Stables - IPGP and Universite Denis Diderot (Paris 7), 2 place Jussieu, 75251 Paris Cedex 05 France (piag@ccr.jussieu.fr)

Catherine Mével
Laboratoire de Petrologie - CNRS UPRES A 7058 Universite Pierre et Marie Curie, Case 110 4 place Jussieu, 75252 Paris Cedex 05 France (mevel@ccr.jussieu.fr)

[1] Analyses of Li and Li isotopes in serpentinized peridotites have been performed using Thermo-Ionisation Mass Spectrometry (TIMS) and Secondary Ion Mass Spectrometry (SIMS) techniques on samples collected from the southwest Indian Ridge (SWIR). In the bulk samples, Li concentrations range from 0.6 to 8.2 ppm, while whole rock δ^6Li values range from −2.9 to −14‰. In situ analyses display a greater range in both Li concentration (0.1–19.5 ppm) and Li isotopic composition (−27 to +19‰), with the serpentinized portions having higher Li concentrations than the associated relict phases. These variations may reflect changes in Li partitioning and isotopic fractionation between serpentine and fluid with temperature and water/rock ratio. They may also be explained by changes in the composition of the serpentinizing fluid over the course of serpentinization. As the serpentine forms by interaction with a circulating fluid, it preferentially removes ^{6}Li, causing the Li in the fluid to become isotopically heavier. The isotopic composition of the initial hydrothermal fluid is dominated by basalt-derived Li, which easily overwhelms the very low Li content originally present in seawater. As this fluid circulates through ultramafic rocks, it induces the formation of serpentine that incorporates this mantle-derived Li. Hence, Li in serpentine is mainly derived from oceanic crust rather than from seawater and serpentinization involves Li recycling within this crust. Consequently, Li isotopes are good tracers of the hydrothermal contribution in serpentinizing fluid. These results imply that serpentinized peridotites are probably only a minor sink of oceanic Li.

Components: 8735 words, 7 figures, 12 tables.

Keywords: Lithium; isotopes; geochemical cycle; oceanic crust; serpentinization.

Index Terms: 0330 Atmospheric Composition and Structure: Geochemical cycles; 1040 Geochemistry: Isotopic composition/chemistry; 1050 Geochemistry: Marine geochemistry.

Received 10 May 2001; **Revised** 9 August 2001; **Accepted** 17 September 2001; **Published** 31 January 2002.

Decitre, S., E. Deloule, L. Reisberg, R. James, P. Agrinier, and C. Mével, Behavior of Li and its isotopes during serpentinization of oceanic peridotites, *Geochem. Geophys. Geosyst.*, *3*(1), 10.1029/2001GC000178, 2002.

1. Introduction

[2] The Li isotopic composition of seawater is homogeneous and well established (δ^6Li = −32.3‰ [*Chan and Edmond*, 1988]). The contributions to seawater Li from rivers and hydrothermal fluids are reasonably well known, but Li removal from seawater during the alteration processes is not completely understood [*Seyfried et al.*, 1984; *Stoffyn-Egli and Mackenzie*, 1984; *Chan et al.*, 1993, 1994; *Huh et al.*, 1998; *Zhang et al.*, 1998]. As serpentinization of peridotites is responsible for an important part of the geochemical transfer between the oceanic lithosphere and seawater, it may affect the Li budget of seawater. This study is the first attempt to understand the Li isotope geochemistry of serpentinized peridotites and to assess the influence of serpentinization on the seawater Li budget. Serpentinization is caused by the interaction between ultramafic rocks and fluid at temperatures below 500°C and high water-rock ratios [*Bonatti et al.*, 1984; *Macdonald and Fyfe*, 1985; *Coulton et al.*, 1995; *McCollom and Shock*, 1998]. Trace elements and stable and radiogenic isotope data argue in favor of seawater derived fluid as the main agent of serpentinization [*Wenner and Taylor*, 1971; *Bonatti et al.*, 1984; *Kimball et al.*, 1985; *Kimball and Gerlach*, 1986; *Agrinier et al.*, 1988; *Früh-Green et al.*, 1996; *Agrinier and Cannat*, 1997]. Nevertheless, fluid chemistry varies with temperature and water-rock ratio [*Kimball and Gerlach*, 1986; *Agrinier et al.*, 1988; *Früh-Green et al.*, 1996]. Consequently, changes in the effect of this fluid on the chemistry of serpentinized rocks may occur during serpentinization. Previous studies have shown that Cl [*Steuber et al.*, 1968; *Rucklidge*, 1972; *Agrinier et al.*, 1988] and B [*Bonatti et al.*, 1984] are incorporated in serpentine. As Li is highly mobile in fluid-related processes such as seafloor alteration [*Seyfried et al.*, 1984; *Stoffyn-Egli and Mackenzie*, 1984; *Chan and Edmond*, 1988; *Chan et al.*, 1992], its concentration in serpentinized peridotites is also expected to change relative to its concentration in unaltered equivalents of these rocks.

[3] Li possesses two stable isotopes, ^{6}Li and ^{7}Li, that can experience extensive fractionation during processes associated with fluid-rock interaction [*Chan and Edmond*, 1988; *Chan et al.*, 1992, 1993, 1994; *You et al.*, 1995]. Previous studies have shown that the Li isotopic signature of seawater (−32.3‰ [*Chan and Edmond*, 1988]) is different from that of basalts (−4.7‰ [*Chan and Edmond*, 1988]) and vent fluids (−6 to −11‰ [*Chan et al.*, 1993]). This suggests that the Li isotopic composition of serpentine may provide clues as to the origin of the serpentinizing fluid. This study focuses on a suite of serpentinized peridotites dredged during the EDUL cruise with R/V *Marion Dufresne* along the southwest Indian Mid-ocean Ridge [*Mével et al.*, 1997]. Our objectives are (1) to determine the origin of Li incorporated in serpentine, in order to evaluate the effect of serpentinization on the seawater Li budget and (2) to investigate Li as an isotopic tracer of serpentinizing fluid composition.

2. Sample Location and Description

[4] The SWIR is an ultra-slow spreading ridge that opens at a half rate of 7–8 mm/yr [*DeMets et al.*, 1990]. This system extends from the Bouvet triple junction northeastward to the central Indian Ocean triple junction. During the EDUL cruise, samples were dredged between 69° and 49°E, and serpenti-

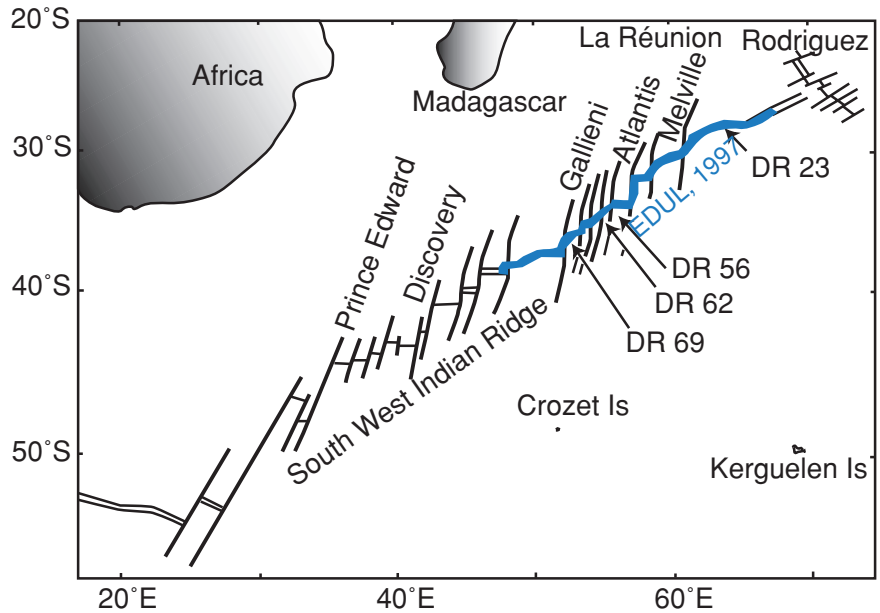

Figure 1. Map of the southwest Indian Ridge showing the locations of dredges from which the samples were obtained.

nized peridotites were sampled along the walls of the rift valley and on the east side of the Gallieni fracture, where the greatest bathymetric depths are attained and the crust is thinnest [*Mével et al.*, 1997]. Samples described in this study were obtained from four different dredges located between 52° and 63°E (Figure 1, Table 1).

[5] These peridotites were originally harzburgites and lherzolites and are partially to completely serpentinized (more than 65 wt% serpentine, Table 2). Relicts of primary phases still present include olivine, orthopyroxene, clinopyroxene, and spinel. The dominant alteration product is serpentine. Minerals stable at higher temperature (amphibole, chlorite) are present in very small amounts in a few samples. The serpentinization process involved the formation of serpentine veins and the hydration of pyroxenes and olivines. Serpentinization of pyroxenes occurred either in fractures or at grain boundaries for the less altered crystals or consisted of the replacement of monocrystals resulting in a bastite texture [*Wicks and Whittaker*, 1977] for the more altered samples. Serpentinization of olivine has produced mesh textures [*Prichard*, 1979] formed by magnetite and serpentine intergrowths with cores of olivine or of serpentine, depending on the degree of serpentinization. In nearly all samples the porphyroblastic texture is preserved, suggesting that serpentinization occurred under static conditions. The only exception is sample DR56 2, which displays a cataclastic texture.

3. Analytical Methods

[6] Whole rock powders of all samples have been analyzed for O and Sr isotopes. Sr

Table 1. Dredge Locations and Depths[a]

	Beginning			End		
	Latitude	Longitude	Depth	Latitude	Longitude	Depth
DR23	28°8.0′S	63°9.7′E	4450	28°7.0′S	63°8.2′E	3950
DR56	34°1.5′S	55°49.7′E	4200	34°2.1′S	55°49.8′E	3750
DR62	34°28.0′S	54°54.0′E	3900	34°27.8′S	54°53.1′E	3500
DR69	36°8.2′S	52°59.6°E	3850	36°7.5′S	53°0.1′E	3800

[a] The locations and depths of the beginnings and the ends of the dredges are indicated.

Table 2. Degree of Serpentinization, Sr, O and Li Isotope Compositions, and Li Contents of the Studied Serpentinized Peridotites[a]

	Serpentinization Degree	Sr, ppm	$^{Sr/86}Sr$ (±2σ)	$\delta^{18}O$, ‰ (±1σ)	$\delta^{18}O$, ‰, Corrected	Serpentinization Temperature, °C	Li, ppm	$\delta^{6}Li$, ‰ (±1σ)	Fractionation Factors	$\delta^{6}Li$, ‰, Fluid
DR23 2-1	72	3.3	0.70880 ± 9	5.20 ± 0.12	5.08	126–175	1.6	−4.2 ± 0.1	1.009–1.011	−13–15
DR23 2-8	82	3.7	0.70867 ± 6	3.24 ± 0.03	2.74	185–262	2.5	−8.1 ± 0.2	1.006–1.009	−14–16
DR23 3-1	94	3.5	0.70934 ± 3	1.63 ± 0.11	1.38	233–345	5.2	−8.5 ± 0.3	1.007	−15–16
DR23 3-5	67	1.0	0.70848 ± 8	2.14 ± 0.12	0.49	275–427	0.6	−12.0 ± 0.2	1.005–1.007	−17–19
DR56 2	85	3.7	0.70838 ± 2	5.77 ± 0.05	5.82	112–155	8.2	−8.6 ± 0.1	1.009–1.011	−17–20
DR56 3	72	2.3	0.70863 ± 4	4.96 ± 0.11	4.75	133–184	2.1	−3.1 ± 0.1	1.008–1.010	−11–13
DR62 4-1	82	3.7	0.70902 ± 3	5.60 ± 0.01	5.62	116–160	4.5	−2.9 ± 0.1	1.009–1.011	−12–14
DR69 1-14	92	1.8	0.70924 ± 5	4.35 ± 0.14	4.25	144–201	3.1	−14 ± 0.3	1.007–1.010	−21–24
Fresh peridotite		1.0	0.7022	5.5			1–3	−4.4–5.5		
Seawater		8.0	0.7092	0			0.19	−32		

[a] The compositions of unaltered peridotites and seawater are indicated for comparison [*Kyser*, 1987; *Ryan and Langmuir*, 1987; *Chan and Edmond*, 1988; *Martin*, 1991; *Brooker et al.*, 2000]. The estimate of the degree of serpentinization is based on major element compositions. Bulk rock $\delta^{18}O$ values are corrected for the proportions of unaltered rock remaining (assuming $\delta^{18}O$ of 5.5‰) to obtain the $\delta^{18}O$ values of the serpentine itself. Serpentinization temperatures are calculated for both open ($\delta^{18}O$ = 0‰) and closed ($\delta^{18}O$ = 2‰) system behavior of the samples. The Li fractionation factors $\alpha_{serpentine\text{-}water}$ were calculated from values $\alpha_{altered\ basalts\text{-}water}$ given by *Chan et al.* [1992], using an exponential interpolation. The fluid isotopic compositions were calculated from the serpentine compositions and the fractionation factors between serpentine and water.

isotopes were determined using a Finnigan MAT262 mass spectrometer after Sr extraction by standard cation exchange techniques. Instrumental mass fractionation was corrected assuming $^{86}Sr/^{88}Sr = 0.1194$. Total blanks were ~300 pg and thus insignificant relative to the quantities of Sr analyzed (10–60 ng). Oxygen isotopic values of bulk serpentinized peridotites were analyzed using well-established analytical methods at Institut de Physique du Globe de Paris (IPGP) (Paris) and are expressed as $\delta^{18}O$ relative to SMOW.

[7] Whole rock Li concentrations were determined by atomic absorption spectrometry following sample digestion in a mixture of HF and $HClO_4$. Whole rock Li isotopic compositions were determined by solid source mass spectrometry at Bristol University following the procedure of *James and Palmer* [2000]. Li was separated from the dissolved sample matrix by cation exchange chromatography. It was then converted to Li phosphate, and isotopic compositions were obtained by measurement of the $^6Li^+$ and $^7Li^+$ beams using a VG336 mass spectrometer. Blanks were ~1.05 ng, which is negligible for a sample size of more than 100 ng Li. The isotopic values are expressed as δ^6Li

$$\delta^6Li = \left\{\left[\left(^6Li/^7Li\right)sample/\left(^6Li/^7Li\right)standard\right] - 1\right\}1000$$

and referenced to the NIST L-SVEC Li_2CO_3 standard. The precision (2σ-m) of these analyses was better than 1‰.

[8] In situ analyses were made using the CRPG Cameca ims3f ion microprobe following a procedure similar to that used for hydrogen [*Deloule et al.*, 1991] and boron isotope [*Chaussidon et al.*, 1997] analyses. Samples were prepared as gold-coated petrographic thin sections. The negative oxygen primary beam, accelerated through 10 kV with 10–20 nA current intensity, was focused to a diameter of 25 μm at the sample surface. Positive secondary ions were accelerated through 4.5 kV.

[9] For concentration determinations, ^7Li and ^{30}Si were measured at a mass resolution of 500 with an energy filtration of 80 ± 10 eV. Secondary ions were counted with an electron multiplier in pulse counting mode. Counting times were 4 s for ^7Li and ^{30}Si over 30 cycles. The nature of the analyzed mineral was determined after each analysis by measuring the intensities of the H, Al, and Ca peaks. In order to obtain Li concentrations, the apparent Li/Si ratios were calculated from ^7Li and ^{30}Si intensities using their atomic masses and isotopic abundances. These apparent Li/Si ratios were then corrected for the relative useful yield (α1) of Li and Si determined on standards during the same analytical session.

$$\alpha 1 = (Li / Si)\ \text{ion microprobe}/(Li/Si)\text{bulk}.$$

[10] The bulk Li/Si ratios obtained by atomic absorption (Li) and electron probe (Si) were taken to represent the true Li/Si ratios of the standards. The standards used were natural minerals containing 1.5–1200 ppm Li. They cover the compositional and structural range encountered in minerals of the samples. Each standard analysis was repeated several times. This allowed us to verify standard homogeneity and to obtain average values. The precision (2σ) obtained on standards is better than 10% for concentrations higher than 5 ppm, and 30% for concentrations lower than 1 ppm. Olivine, pyroxenes, biotite, amphibole, and basalt plot on a single line, demonstrating the absence of large matrix effects on Li ion yield (Figure 2, Table 3). The serpentine standard UB-N plots significantly off this line, but this almost certainly reflects the great heterogeneity of Li in serpentine, described below, rather than a matrix effect. This explanation is especially likely since the bulk concentration was obtained from a powder homogenized from several kg of rock, while the point analyses represent only several nanograms of material sputtered from grains taken from a different portion of the rock. Li content in this unpowdered portion may be unrepresentative of the UB-N serpentine powder, and therefore it was not considered as a standard.

[11] The precision on the determination of the coefficient α1 ranges between 10 and 15%,

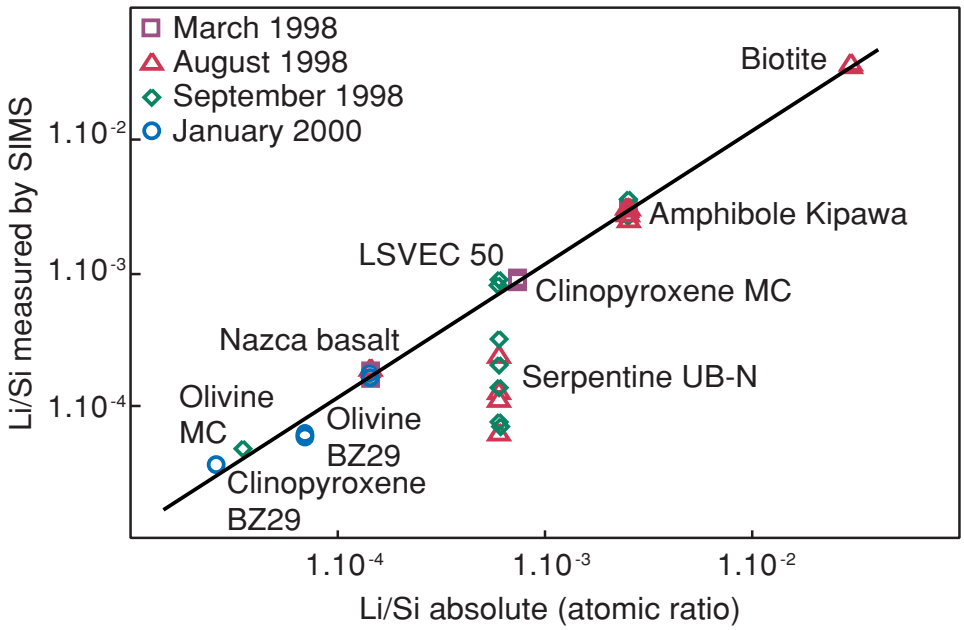

Figure 2. Ion yield calibration curves of standards for four different analytical sessions: Li/Si measured by ion microprobe versus Li/Si measured on bulk powders by conventional methods. Standards are biotite from the Massif Central (France), clinopyroxene BZ29 and olivine BZ29 separates from Zabargad lherzolite (provided by R. Brooker), clinopyroxene MC and olivine MC from the Massif Central (France), and amphibole from Kipawa and serpentine UB-N from the Vosges. This last standard was highly irreproducible for reasons discussed in the text and therefore was not included in the calculation of the regression lines. The slopes of the lines are 1.218 ± 0.006 (September 1998), 1.228 ± 0.028 (March 1998), 1.276 ± 0.005 (August 1998), and 1.138 ± 0.089 (January 2000) and the intercepts are 0.0001, 0.0001, -5.10^{-5}, and -2.10^{-6}, respectively. The slopes of the lines represent the α_1 values. Analyses of basaltic glass from Nazca are also shown. The Li content of this basalt was calculated for three different sessions: 9.9 ppm (March 1998), 10.1 ppm (August 1998), 9.5 ppm (January 2000).

including the matrix effect between the different mineral species. The variation of the coefficient $\alpha 1$ between sessions, owing to variations in the instrumental set-up and ion multiplier aging, is less than 15%. Thus all of the coefficients $\alpha 1$ were within error and so do not bias the corrected Li contents beyond the calculated uncertainties. This is shown by replicate analyses of the same sample, such as the Nazca basalt in Figure 2. The agreement between the weighted averages of the in situ measurements and the corresponding whole rock measurements of the different samples indicates that our calibration did not introduce any large bias in the results.

[12] For isotopic analyses the mass resolution was set at 1100, allowing the separation of ^{6}LiH from ^{7}Li. Therefore no energy offset was applied, and the energy slit was kept wide open. The 20 μm spot was centered in a 150 μm aperture. The ^{6}Li and ^{7}Li were measured for 6s and 3s, respectively, over 120 peak jumping cycles, with magnetic field repositioning every 10 cycles. The isotopic instrumental fractionation was monitored by measuring several standards. Such fractionation may result from instrumental parameters or from matrix effects, that is, variations in sample composition and structure [*Deloule et al.*, 1992]. The ion probe ^{6}Li/^{7}Li measurements of standards, expressed in δ notation relative to the LSVEC ^{6}Li/^{7}Li ratio (0.0832) [*Flesch et al.*, 1973], are plotted in Figure 3 against their δ^6Li values measured by TIMS. Standards with δ^6Li ranging from −10 to +4‰ plot on a single line with a slope of 1, demonstrating the absence of any matrix effect on the Li instrumental isotopic fractionation in our

Table 3. Li/Si Atomic Ratios Calculated From $^{7}Li/^{30}Si$ Measured by Ion Microprobe for Mineral Standards Compared to Li/Si Ratios Measured by Conventional Techniques for Four Different Analytical Sessions[a]

	Li/Si True	Li/Si Measured			
		Sept. 1998	March 1998	Aug. 1998	Jan. 2000
Serpentine UB-N	5.93×10^{-4}	1.38×10^{-4}		1.30×10^{-4}	
		2.08×10^{-4}		2.39×10^{-4}	
		7.11×10^{-5}		1.13×10^{-4}	
		7.65×10^{-5}		6.28×10^{-5}	
		3.14×10^{-4}			
Average		1.61×10^{-4}		1.36×10^{-4}	
Pyroxene MC	5.92×10^{-4}	8.13×10^{-4}			
		8.75×10^{-4}			
		8.03×10^{-4}			
Average		8.30×10^{-4}			
Olivine MC	3.46×10^{-5}	4.57×10^{-5}			
		4.91×10^{-5}			
Average		4.74×10^{-5}			
Amphibole Kipawa	2.60×10^{-3}	3.67×10^{-3}	3.17×10^{-3}	3.18×10^{-3}	
		3.19×10^{-3}		3.32×10^{-3}	
		2.65×10^{-3}		3.14×10^{-3}	
				2.58×10^{-3}	
				2.84×10^{-3}	
Average		3.17×10^{-3}	3.60×10^{-3}	3.01×10^{-3}	
Biotite	3.02×10^{-2}		3.72×10^{-2}	3.88×10^{-2}	
			3.79×10^{-2}	3.82×10^{-2}	
			3.65×10^{-2}	3.91×10^{-2}	
				3.77×10^{-2}	
				3.88×10^{-2}	
Average		3.72×10^{-2}	3.72×10^{-2}	3.85×10^{-2}	
LSVEC50	7.47×10^{-4}		9.04×10^{-4}		
			9.00×10^{-4}		
			8.64×10^{-4}		
Average			8.89×10^{-4}		
Nazca basalt	1.42×10^{-4}		1.81×10^{-4}	1.87×10^{-4}	1.72×10^{-4}
			1.64×10^{-4}	1.91×10^{-4}	1.59×10^{-4}
			1.69×10^{-4}	1.91×10^{-4}	
Average			1.71×10^{-4}	1.89×10^{-4}	1.65×10^{-4}
Cpx BZ29	2.55×10^{-5}				3.58×10^{-5}
Average					3.58×10^{-5}
Olivine BZ29	6.94×10^{-5}				5.66×10^{-5}
					6.71×10^{-5}
Average					6.19×10^{-5}

[a] Each value represents a single analysis.

instrumental set up. This allows us to apply the same correction regardless of the mineral analyzed. The instrumental mass fractionation is expressed in $\delta^{6}Li$ units:

$$\Delta i = \left(\delta^{6}\mathrm{Li}\right)\text{ ion microprobe} - \left(\delta^{6}\mathrm{Li}\right)\text{ mass spectrometer.}$$

In applying the Δi value determined on BHV0 (basaltic glass, international standard) to the other standards, all the ion probe values are within error of the TIMS values (Table 4). The value of Δi may change between different sessions, owing to variations in the ion probe set up and to electron multiplier aging [*Deloule et al.*, 1992]. Therefore BHV0 was used as an internal reference and measured systematically before and after each sample to monitor the Δi value. The reproducibility (2σ-m) of the BHV0 analyses during an analytical session was better than 2‰. To further test the method we measured $\delta^{6}Li$ in pyroxene in a fresh continental

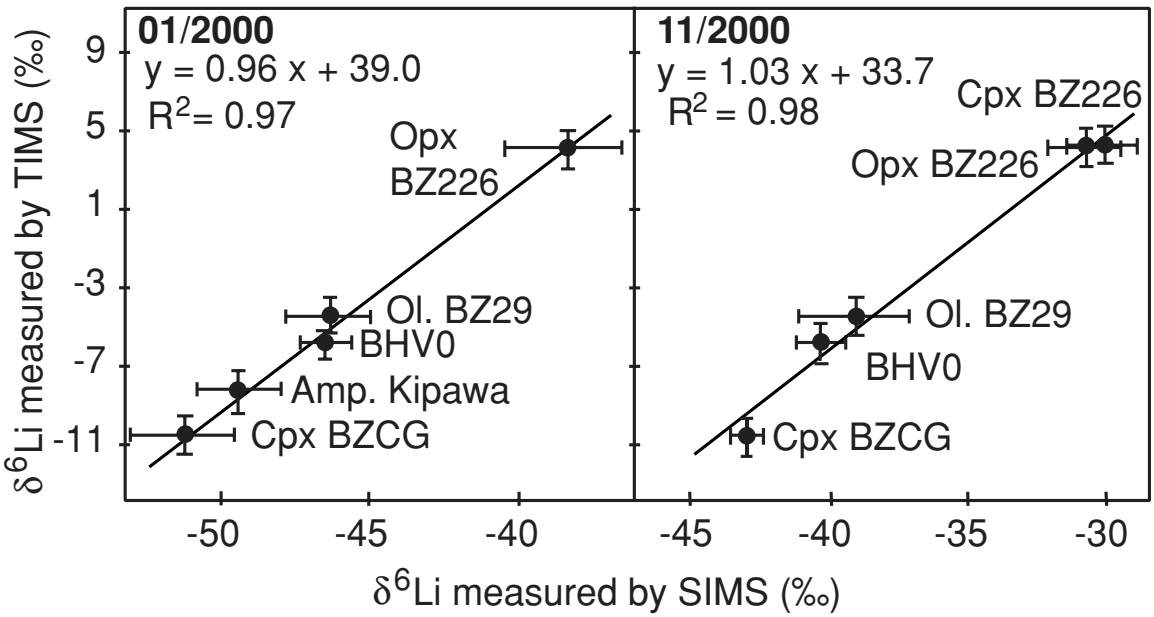

Figure 3. The δ^6Li measured by TIMS (Bristol University) versus δ^6Li measured by ion microprobe for the standards previously described in Figure 2. In each session standards fall on a line with a slope within uncertainty of 1, demonstrating the lack of a matrix effect. The variation of ion probe instrumental fractionation (δ^6Li by SIMS - δ^6Li by TIMS) between sessions is due to variation in the instrumental set-up, mainly electron multiplier aging.

peridotite xenolith. The reproducibility of the results (Figure 4, δ^6Li = 2.7 ± 1.7‰ over 10 measurements) demonstrates the reliability of the in situ isotopic measurements.

4. Results

4.1. Sr and O Isotopes

[13] The ^{87}Sr/^{86}Sr ratios range from 0.70838 to 0.70934 (Table 2), suggesting high water/rock ratios and interaction with fluids dominated by seawater. The δ^{18}O values of our samples range between 1.63 and 5.77‰ (Table 2). The δ^{18}O values of the serpentine itself were determined by correcting for the proportions of unaltered rock remaining, assuming a δ^{18}O of 5.5‰ for fresh peridotite. These corrected values were used to determine serpentinization temperatures [*Bonatti et al.*, 1984]. Assuming that the serpentinizing fluid may be either seawater (δ^{18}O = 0‰) or a

Table 4. Results of Standard Analyses For Two Different Analytical Sessions: δ^6Li values Measured By SIMS Compared to Compositions Measured By Thermal Ionization Mass Spectrometry (TIMS)[a]

Samples	First Session			Second Session			TIMS Values (±1‰)
	N	δ^6Li (‰) SIMS Values ±(2 σ/√*n*)		*N*	δ^6Li (‰) SIMS Values ±(2 σ/√*n*)		
		Measured	Corrected		Measured	Corrected	
BHV0	2	−46.3	−5.8 ± 1.0	3	−40.3	−5.8 ± 0.4	−5.8
Opx BZ226	4	−38.1	2.3 ± 2.0	4	−30.2	4.3 ± 1.3	4.2
Olivine BZ29	4	−46.2	−5.7 ± 1.4	7	−39.1	−4.6 ± 2.0	−4.6
Cpx BZ226	6	−34.9	5.5 ± 1.4	3	−30.8	3.7 ± 1.3	4.1
Cpx BZCG	2	−51.2	−10.7 ± 1.7	4	−43.0	−8.5 ± 0.6	−10.5
Amphibole Kip.	3	−49.3	−8.8 ± 1.5				−8.2

[a] Each value represents the average of several determinations (number of analyses *N* given in the table). Standards are as follows: Olivine BZ29 separates from Zabargad lherzolite; Opx BZ226 and Cpx BZ226 separates from Zabargad pyroxenite; Cpx BZCG separates from Zabargad pyroxenite (provided by R. Brooker); Amphibole separates from Kipawa; and BHV0 basaltic glass separates from Hawaï (Li composition reported in *James and Palmer* [2000]). All results are normalized to the NIST L-SVEC Li_2CO_3.

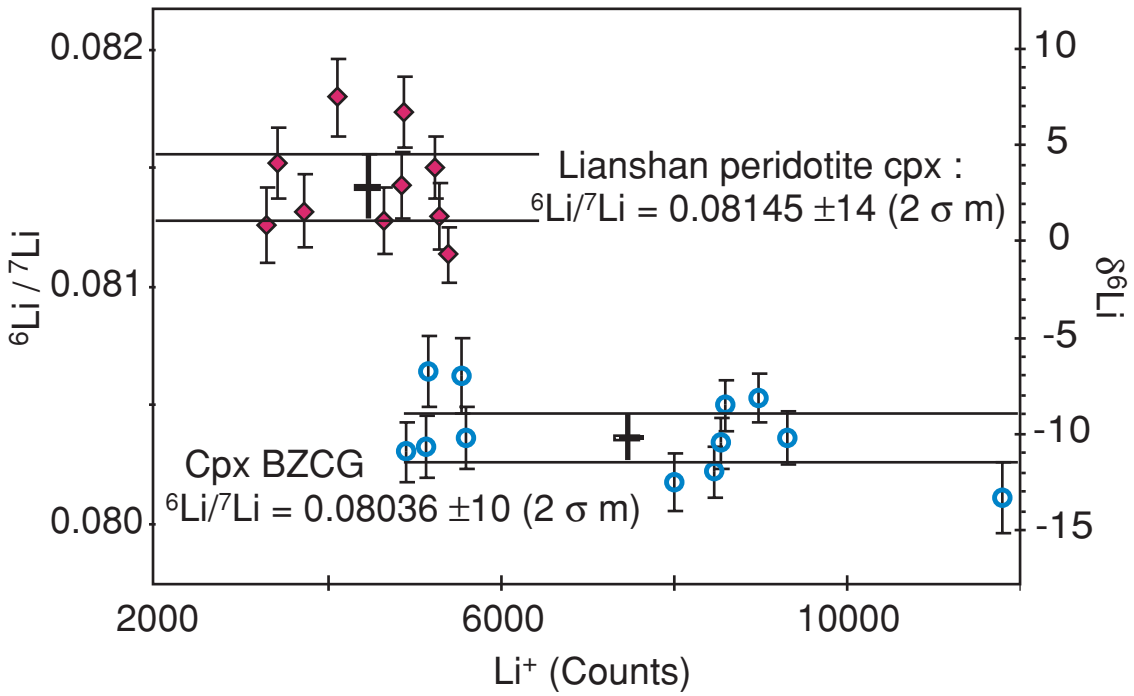

Figure 4. Repeated ion probe measurements of Li isotopic composition of a continental peridotite cpx and of the standard cpx BZCG [*James et al.*, 1995].

seawater-derived fluid ($\delta^{18}O$ = 2‰), the oxygen isotope temperature relationship between water and serpentine reported by *Wenner and Taylor* [1971] yields serpentinization temperatures between 100° and 430°C (Table 2).

4.2. Li Contents

[14] The serpentinized peridotites contain between 0.6 and 8.2 ppm Li (Table 2). Their Li concentration increases with serpentinization degree and is on average higher than that of fresh peridotites (1–3 ppm [*Ryan and Langmuir*, 1987, *Seitz and Woodland*, 2000]). The cataclastic sample DR56 2 is enriched in Li (8.2 ppm) relative to the other samples despite the fact that its serpentinization degree and $^{87}Sr/^{86}Sr$ ratio are not the highest.

[15] All point analyses are reported in Tables 5–12, and those from four thin sections are

Table 5. Li Contents and Isotopic Compositions "In Situ" Measurements on Serpentine and Relict Phases From Peridotite DR56 3

	Relicts opx		Relicts cpx		Relicts ol		Serp opx		Serp cpx		Serp ol		Serp Veins	
	δ^6Li, ‰	Li, ppm	δ^6Li, ‰	Li, ppm	δ^6Li, ‰	Li, ppm	δ^6Li, ‰	Li, ppm	δ^6Li, ‰	Li, ppm	δ^6Li, ‰	Li, ppm	δ^6Li, ‰	Li, ppm
DR56 3	−3.4	0.9	−17.1	0.1	−26.9	1.0	−19.1	1.3	−2.0	2.5	−12.8	19.5	−1.9	7.3
	−2.7	1.3					−15.5	4.3			−15.7	4.5	−1.4	14.2
	−0.2	0.5					−17.1	5.7			−2.9	7.7	−5.2	1.2
	−17.0	0.5					−4.2	6.7			0.5	2.9	−13.7	0.7
	−14.0	0.2					8.1	16.0			−20.7	1.3	−14.3	1.1
	−21.6	0.5					2.4	17.5			3.3	4.8	2.0	3.0
							−4.0	10.1			−14.6	6.5	5.2	2.2
							−6.8	11.7						
							8.4	1.7						
							7.3	1.2						
							5.8	1.1						
Average	−9.8	0.7	−17.1	0.1	−26.9	0.7	−3.1	7.0	−2.0	2.6	−9.0	6.7	−4.2	4.2

Table 6. Li Contents and Isotopic Compositions "In Situ" Measurements on Serpentine and Relict Phases From Peridotite DR23 2-1

	Relicts opx		Relicts cpx		Relicts ol		Serp opx		Serp cpx		Serp ol		Serp Veins	
	δ^6Li, ‰	Li, ppm	δ^6Li, ‰	Li, ppm	δ^6Li, ‰	Li, ppm	δ^6Li, ‰	Li, ppm	δ^6Li, ‰	Li, ppm	δ^6Li, ‰	Li, ppm	δ^6Li, ‰	Li, ppm
DR23 2-1	−8.6	0.7			−18.3	1.0	−1.1	1.9			−5.6	1.1	−18.7	2.4
	−16.4	0.5			−17.2	0.9	−0.6	1.3			−5.4	1.5	−2.3	2.1
	−10.9	0.6									−0.2	0.9		
	−9.5	0.9									−10.3	1.0		
	−15.2	0.6												
Average	−12.1	0.7			−17.8	0.9	−0.9	1.6			−5.4	1.1	−10.5	2.2

shown in Figure 5. Relict minerals have very low Li contents with an average of 0.8 ± 0.3 ppm for olivines, 0.7 ± 0.2 ppm for orthopyroxenes, and 1.1 ± 0.6 ppm for clinopyroxenes. In the two samples with more than one relict clinopyroxene datum, clinopyroxene Li concentrations are about twice those of orthopyroxene. Li contents reported by *Ryan and Langmuir* [1987] for fresh olivine and pyroxene separates are higher (1.4–4 ppm). It is possible that this difference reflects higher degrees of melt extraction in our samples or metasomatic enrichment of the samples analyzed by the other authors. However, it may also imply that Li loss from relict phases occurs during alteration. This is further suggested by the heterogeneity of the Li concentration of relict phases within individual samples, which exceeds the reproducibility of standards of similar concentration. It would not be surprising, considering the extent of serpentinization, for relict minerals to be affected by alteration even if they appear optically fresh.

[16] Serpentine contains considerably more Li than relict minerals, with an average content of 4 ppm. The total range of values is large: from 0.1 to 19.5 ppm. These analyses show that the Li distribution is heterogeneous in serpentinized peridotites and that Li is generally enriched in serpentine compared to relict minerals. The least serpentinized sample (DR23 3−5) is Li-depleted and contains Li-poor serpentine. This suggests that bulk Li content is dependent not only on the degree of serpentinization but also on the degree of Li incorporation in serpentine.

Table 7. Li Contents and Isotopic Compositions "In Situ" Measurements on Serpentine and Relict Phases From Peridotite DR62 4-1

	Relicts opx		Relicts cpx		Relicts ol		Serp opx		Serp cpx		Serp ol	
	δ^6Li, ‰	Li, ppm	δ^6Li, ‰	Li, ppm	δ^6Li, ‰	Li, ppm	δ^6Li, ‰	Li, ppm	δ^6Li, ‰	Li, ppm	δ^6Li, ‰	Li, ppm
DR62 4-1	−9.3	1.0	−23.3	1.9			5.7	4.5	−8.6	1.9	−6.5	0.9
	−4.8	0.7	−17.6	1.6			4.6	6.2	−2.2	2.5	8.3	1.1
	−17.3	0.6					19.1	6.7	−7.4	4.4	−6.6	0.7
	−4.4	1.0					−7.9	5.1	−2.1	4.6	−3.7	3.0
							1.0	7.7	7.5	3.5	−25.5	0.7
									−10.5	5.9	0.5	1.7
											−5.4	5.3
											5.4	1.7
											17.0	7.4
Average	−8.9	0.8	−20.5	1.8			0.8	5.9	−3.9	3.8	−1.1	2.0

Table 8. Li Contents and Isotopic Compositions "In Situ" Measurements on Serpentine and Relict Phases From Peridotite DR23 3-5

	Relicts opx		Relicts cpx		Relicts ol		Serp opx		Serp ol		Chlorite	
	δ^6Li, ‰	Li, ppm	δ^6Li, ‰	Li, ppm	δ^6Li, ‰	Li, ppm	δ^6Li, ‰	Li, ppm	δ^6Li, ‰	Li, ppm	δ^6Li, ‰	Li, ppm
DR23 3-5	−5.2	0.4			−8.1	0.3	−15.9	0.1	−19.4	0.0	8.9	0.2
	−14.2	0.6			−13.3	0.5	−4.6	0.2			−23.7	0.2
	0.1	0.5			−10.5	0.7	−13.7	0.1				
							−2.3	0.2				
							−3.2	2.9				
							16.2	1.0				
Average	−6.4	0.5			−10.6	0.5	−7.9	0.7	−19.4	0.0	−7.4	0.2

[17] Amphiboles, analyzed only in sample DR23 2−8, have an average Li content of 1.6 ppm. Chlorite in sample DR23 3−5 is low in Li (0.2 ppm), while that from sample DR56 2 is high in Li (12.2 ± 7.1 ppm). The serpentine Li content is similar to that of the associated chlorite (0.2 ppm in DR23 3−5 and 4−20 ppm in DR56 2). Few measurements were performed on amphibole, but they show that the amphibole Li content is close to that of the serpentine in the sample DR23 2−8 (1−2 ppm). No clear relationship between the type of alteration phase and the Li content is found.

4.3. Li Isotopes

[18] The Li isotope composition of whole rocks ranges between −14 and −2.9‰ (Table 2). No correlation is observed between the whole rock δ^6Li and Li content. The few data from fresh peridotites that exist [*Brooker et al.*, 2000] give δ^6Li values between −4.4 and −5.5‰, which is consistent with the mantle value inferred from fresh mid-ocean ridge basalt (MORB) [*Chan et al.*, 1992]. Hence five of our samples are isotopically heavier, and three samples are similar to or slightly lighter than unaltered peridotites.

[19] In situ isotopic analyses show that δ^6Li values vary greatly, between −27 and +4‰ for relict minerals, and between −25 and +19‰ for serpentine (Table 5; Figure 6). The variation observed within relict phases of individual samples (up to ±10‰) is much greater than that observed in repeated measurements of standards and of pyrox-

Table 9. Li Contents and Isotopic Compositions "In Situ" Measurements on Serpentine and Relict Phases From Peridotite DR23 2-8

	Relicts opx		Relicts cpx		Relicts ol		Serp opx		Serp ol		Chlorite	
	δ^6Li, ‰	Li, ppm	δ^6Li, ‰	Li, ppm	δ^6Li, ‰	Li, ppm	δ^6Li, ‰	Li, ppm	δ^6Li, ‰	Li, ppm	δ^6Li, ‰	Li, ppm
DR23 2-8	−4.9	0.6	−10.3	1.1			6.7	7.6	−3.7	1.0	−2.6	1.1
	−6.0	0.5	−5.3	0.5			7.5	3.3	2.6	1.1	11.1	2.1
	−7.4	0.6	4.1	1.0			2.3	3.4	−3.9	1.1		
	−0.5	0.6	3.4	1.3			13.3	8.7	−7.2	0.8		
	−8.3	0.6	−4.4	1.4			4.8	4.5	4.4	0.7		
							−3.0	4.4	−4.4	0.6		
							−1.8	1.9				
							9.9	4.5				
							−1.5	2.3				
							−3.6	1.1				
							0.3	2.0				
							6.7	5.8				
Average	−5.4	0.6	−2.5	1.1			2.6	3.7	−2.0	0.9	4.3	1.6

Table 10. Li Contents and Isotopic Compositions "In Situ" Measurements on Serpentine and Relict Phases From Peridotite DR23 3-1

	Serp opx		Serp ol	
	δ^6Li, ‰	Li, ppm	δ^6Li, ‰	Li, ppm
DR23 3-1	−14.5	2.0	−3.9	6.0
	−22.9	2.4	−17.5	5.1
			−14.1	6.3
			−21.4	1.9
			−6.8	0.2
			−11.3	0.6
			−0.3	5.3
			−11.8	5.1
Average	−18.7	2.2	−10.9	3.8

ene from a fresh continental peridotite (±2‰, see section 3). The average values of relict minerals (−8.8 ± 10‰ for relict pyroxenes and −15.7 ± 7‰ for relict olivines) are more negative than the values reported for fresh peridotite phases (−4 to −7‰ [*Brooker et al.*, 2000]) and for MORB (−4 to −6‰ [*Chan and Edmond*, 1988; *Chan et al.*, 1993]). Within individual mineral grains, there is a general tendency for spots with higher Li contents to have higher δ^6Li (Figure 5). The low average δ^6Li values and the large range of variation observed within the relict phases of individual samples, indicate that their Li isotopic compositions were modified during hydrothermal alteration. The averages of the point analyses for each sample, including both relict and serpentinized phases, are in most cases similar to the values obtained for the corresponding bulk rock. An exact equivalence is not expected because in situ averages truly representative of bulk rock compositions require a much larger number of analyses and because other minor phases that were not analyzed may be present. The primary aim of the in situ analyses was to compare compositions of altered and relict minerals, rather than to estimate the bulk rock composition. Amphiboles analyzed in sample DR23 8 have an average value of +4.3 ± 9.7‰ and chlorites in samples DR23 3–5 and DR56 2 of −7.7 ± 10.7‰. However, as these are minor phases and as only a few analyses were performed, they may be not representative.

5. Discussion

5.1. Whole Rock Li Systematics

5.1.1. Li enrichment in serpentinized peridotites

[20] The whole rock analyses show that overall Li is more concentrated in serpentinized peri-

Table 11. Li Contents and Isotopic Compositions "In Situ" Measurements on Serpentine and Relict Phases From Peridotite DR69 1-14

	Serp opx		Serp ol	
	δ^6Li, ‰	Li, ppm	δ^6Li, ‰	Li, ppm
DR69 1-14	−6.1	5.1	−18.7	1.0
	−1.2	6.1	−17.3	1.3
	−15.9	7.6		
	−12.6	7.7		
	−15.0	7.6		
Average	−10.2	6.8	−18.0	1.2

Table 12. Li Contents and Isotopic Compositions "In Situ" Measurements on Serpentine and Relict Phases From Peridotite DR56 2

	Serp opx		Serp ol		Chlorite	
	δ^6Li, ‰	Li, ppm	δ^6Li, ‰	Li, ppm	δ^6Li, ‰	Li, ppm
DR56 2	2.9	14.5	3.6	3.3	−13.1	4.6
	4.0	7.2	−5.5	4.9	−6.5	10.5
	3.9	6.7	−11.4	3.8	−7.5	12.0
	−5.9		−6.6	3.9	−4.4	21.7
	−1.0					
	−2.9					
	2.6	15.1				
	7.5	10.5				
	−3.3	4.0				
	−0.8	4.0				
Average	0.7	8.9	−5.0	4.0	−7.9	12.2

dotites than in fresh peridotite. The Li content is lowest in the sample DR23 3–5 (0.6 ppm), formed at the highest temperature (240°–360°C), and higher in the other samples (up to 8.2 ppm), formed at lower temperatures. Assuming that Li behavior during serpentinization is analogous to that during basalt alteration, this observation is consistent with experimental studies of *Seyfried et al.* [1984] and *Berger et al.* [1988] that show that Li is incorporated in smectites and chlorites at low temperatures (<150°C), in increasing amounts with increasing water/rock ratio, and conversely is extracted from the basalt into solution, at high temperatures (>250°C). Relatively high Li contents in serpentinized peridotites may also result from high Li contents in the fluid. The Li contents of vent fluids at high temperature (6–9 ppm [*Edmond et al.*, 1979; *Von Damm et al.*, 1983]) are much higher than that of seawater (0.19 ppm [*Morozov*, 1968]). Thus the implication of such fluids in the serpentinization process can contribute to the higher Li content of serpentine.

5.1.2. Li isotopic composition of serpentinized peridotites: Effects of fluid evolution

[21] Whole rock δ^6Li values range from −2.9‰ (close to MORB or fresh peridotites) to −14‰. Because serpentine is the dominant mineral in these samples, the whole rock Li compositions should reflect those of the corresponding serpentine. The isotopic composition of Li carried by the serpentinizing fluid can be estimated from the δ^6Li values of serpentine and the temperature dependent serpentine-fluid isotopic fractionation factor. Isotopic fractionation factors $\alpha_{\text{mineral-water}}$ between altered basalts and water, empirically derived by *Chan et al.* [1992], vary from 1.004 at 300°C to 1.012 at 100°C. We assume as a first approximation that isotopic fractionation during uptake of Li by serpentine is similar to that during uptake of Li by altered basalts. The calculated δ^6Li values of the serpentinizing fluid range between −11 and −24‰ (Table 2). These compositions are intermediate between those of vent fluid (−6 to −11‰ [*Chan et al.*, 1993]) and seawater (−32.3‰ [*Chan and Edmond*, 1988]).

[22] The model we propose to explain these values is illustrated in Figure 7. The high Cl contents of the oceanic serpentinized peridotites suggest that the fluid was originally seawater [*Anselmi et al.*, 2000]. Seawater is highly depleted in Li and especially in ^{6}Li (Li = 0.18 ppm and δ^6Li = −32.3‰ [*Chan and Edmond*, 1988]). As seawater penetrates into the oceanic crust and heats up, its Li signature quickly becomes dominated by Li derived from the basalt with which it interacts. This signa-

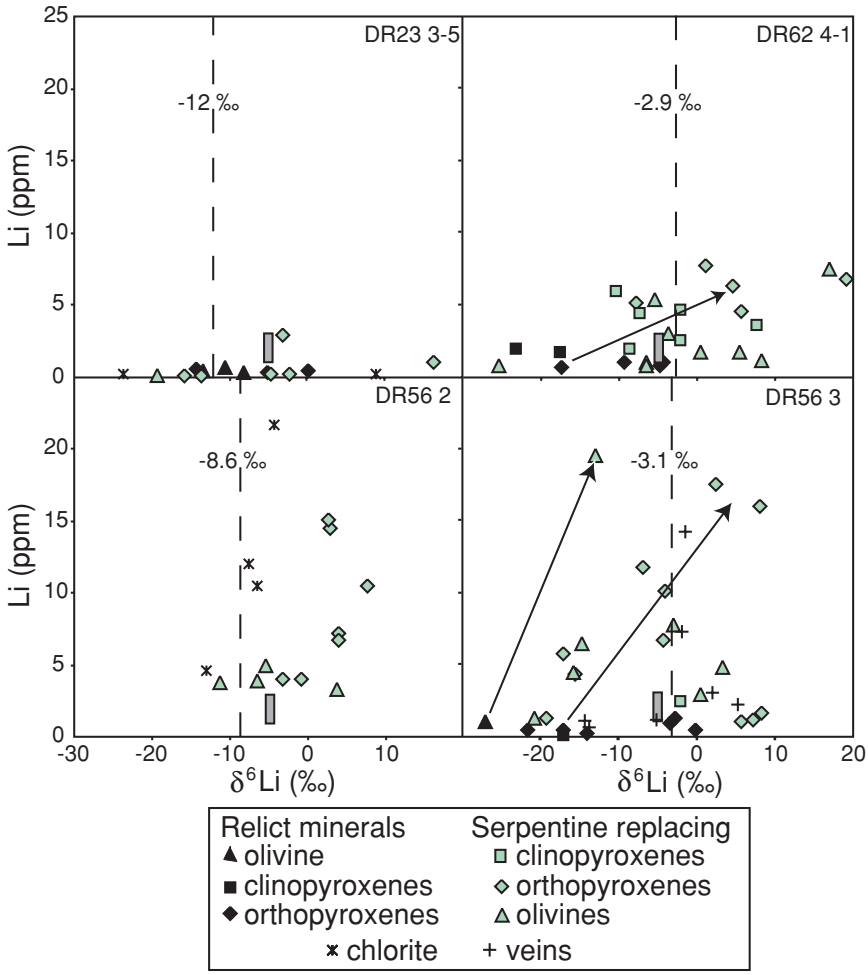

Figure 5. Variations of Li contents versus Li isotopic compositions measured in situ for four samples. The gray square indicates the composition of fresh peridotites [*Brooker et al.*, 2000]. Dashed lines denote the whole rock isotopic compositions. Arrows connect serpentinized and unserpentinized portions of single mineral grains, indicating a tendency for spots with high Li contents to have high δ^6Li values. The high heterogeneity in Li content and isotopic composition indicates that serpentine is not in equilibrium within each individual sample.

ture is indeed observed in fluids sampled from black smokers (δ^6Li between -6 and -10‰, Li concentration $\sim$10 ppm [*Chan et al.*, 1993, 1994]). As this fluid continues to circulate deeper into the ocean crust, it provokes the formation of serpentine. This serpentine incorporates Li, preferentially ^{6}Li. Serpentine formed early in this process will have relatively high δ^6Li. In fact, this early-formed serpentine may have δ^6Li values even higher than those of fresh basaltic crust. The temperature of formation of secondary minerals is lower than the temperature of extraction of Li. Therefore the fluid-mineral isotopic fractionation factor during serpentine formation may be up to 10‰ higher than that during Li extraction from basalt. So serpentine formed from a fluid that interacted with basalt at high temperature may have higher δ^6Li values than the basalt. Furthermore during the extraction process the δ^6Li values of the altered basalt will increase progressively [*Chan et al*, 1998]. Thus the fluids that interact with these altered basalts will also have increasingly higher δ^6Li values, allowing the formation of serpentine with still higher δ^6Li.

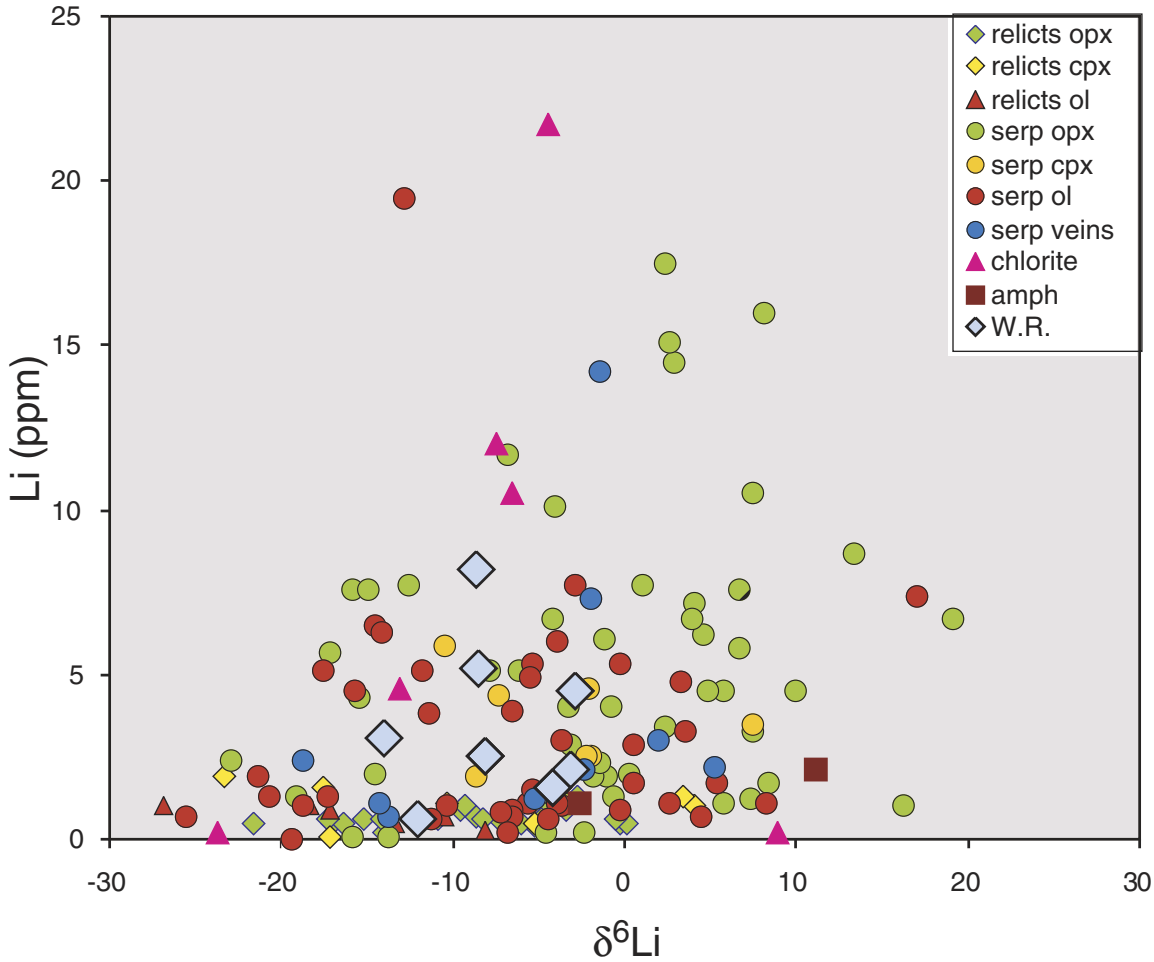

Figure 6. Li contents versus Li isotopic compositions measured in situ for all samples and for whole rock analysis.

[23] In contrast, the serpentine formed later on the hydrothermal fluid circulation path will have lower δ^6Li values reflecting derivation from more evolved fluids (Figure 7). As ^{6}Li is preferentially removed during serpentinization, the δ^6Li of the hydrothermal fluid evolves toward lower values during its passage through the oceanic crust, following a process roughly analogous to Rayleigh fractionation. The final fluids expelled from serpentinized peridotites should thus be depleted in Li and have more negative isotopic compositions than hydrothermal vent fluids. The highly ^{6}Li-depleted fluid compositions and the highly ^{6}Li-enriched fluid compositions are obtained at the extremes of two different distillation processes, reflecting respectively ^{6}Li incorporation during serpentinization at decreasing temperature and progressive leaching of ^{7}Li from basalts at high temperature. Thus these extreme values should be less commonly observed than the intermediate values, close to the initial basalt composition. The weighted mean δ^6Li value of our samples is −7.6‰, close to the range of oceanic basalt.

[24] This scenario suggests that Li incorporated in serpentine is ultimately derived from leaching of basalt and peridotite at high temperature. Thus serpentinization implies Li transfer from hydrothermal fluid to peridotite as the fluid cools and involves primarily a redistribution of Li within the oceanic crust. For this reason, serpentinized peridotites are probably only a minor sink of oceanic Li. Furthermore, the

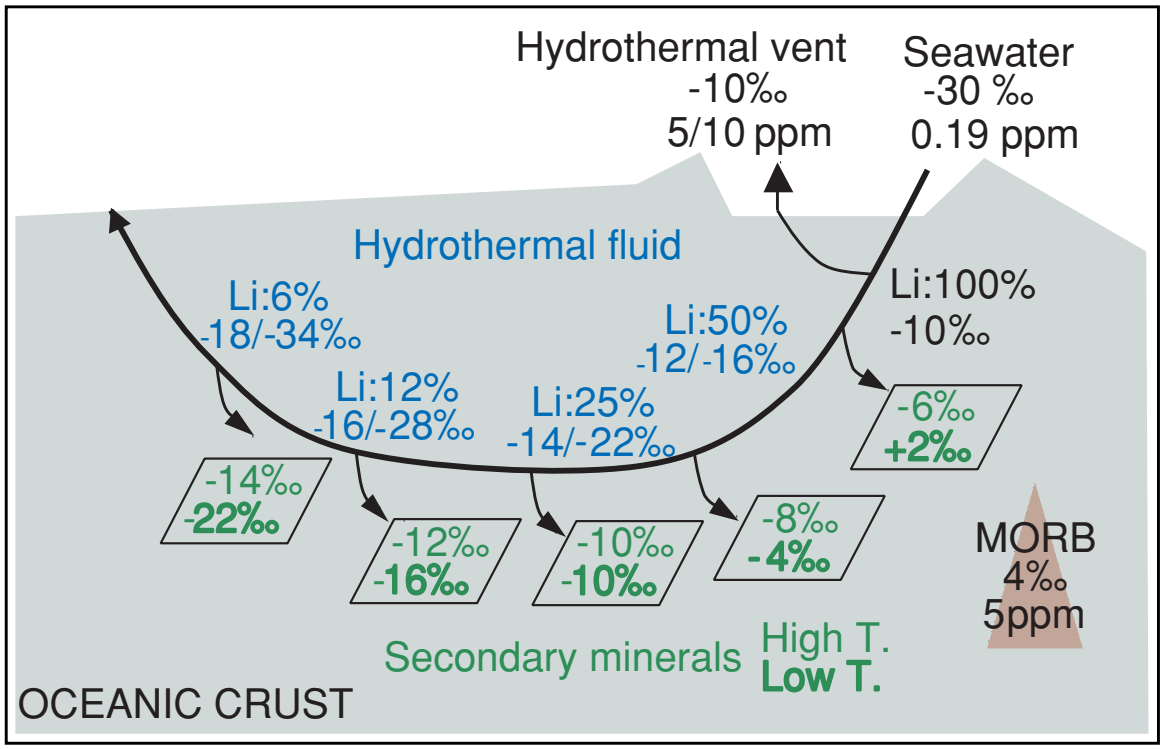

Figure 7. Schematic representation of the evolution of the Li content and isotopic composition of hydrothermal fluid and the Li isotopic composition of secondary minerals formed during the interaction of the fluid with the peridotite. The initial fluid is considered to be similar to high temperature vent fluids. For each step, we assume for simplicity that 50% of the Li in the fluid is taken up by the secondary minerals. In reality the partition coefficient will change with temperature. The isotopic fractionation factor between fluid and minerals may range from 1.004 to 1.012, depending on the temperature of the fluid [*Chan et al.*, 1992]. Therefore the δ^6Li values given for each step represent the upper and lower bounds.

expelled late stage fluids will have little effect on the δ^6Li of seawater, both because they should have low Li concentrations and because their isotopic compositions will probably have evolved to values similar to that of seawater.

5.1.3. Combined Li-Sr-O Isotopic Systematics

[25] Examination of the data in Table 2 suggests that there is no simple relationship between Li, Sr, and O isotopic systematics. In large part this may reflect the fact that these samples were separated by large distances (hundreds of kilometers) and represent several tectonic units. The absence of any correlation between Li and Sr contents and isotopic compositions in our data may also suggest that Li and Sr have very different behaviors during serpentinization. We cannot compare the behavior of these elements on a small scale because in situ analyses of Sr isotopic compositions are not available. Nevertheless we can consider that the whole rock compositions represent averages of serpentine formed under variable temperature conditions and water/rock ratios and which has exchanged with fluids having variable compositions.

[26] In our Li modeling, we suggest that the main source of Li in serpentine is hydrothermal fluid that has acquired the Li signature of the basaltic crust. Indeed such fluids display high Li contents, with high δ^6Li [*Chan et al.*, 1993] consistent with a derivation from leaching of basaltic crust. These fluids also have Sr isotopic compositions marked by the oceanic crust, with

low $^{87}Sr/^{86}Sr$ (0.703–0.704) but with Sr contents (3.5–7 ppm) [*James et al.*, 1995] lower than or equal to that of seawater. As these fluids circulate through the peridotite provoking serpentinization they will evolve and deposit Li with variable isotopic compositions, as described in section 5.1.2. However, while the high temperature hydrothermal fluids may deposit Sr, they will have little effect on the Sr isotopic compositions of the peridotites, since these originally have comparable $^{87}Sr/^{86}Sr$ ratios. Nevertheless, the serpentines now have very radiogenic Sr compositions ($^{87}Sr/^{86}Sr > 0.7084$). This suggests that the original Sr compositions existing after high temperature fluid circulation were overprinted by interaction with low temperature fluids dominated by seawater at or near the seafloor surface. A similar overprinting process has been observed in anhydrite from the TAG hydrothermal mound, on the Mid Atlantic Ridge [*Teagle et al.*, 1998]. The crucial difference between Li and Sr systematics is that seawater is rich in Sr but poor in Li. As seawater has a very low Li concentration (0.19 ppm), much lower than that of hydrothermal fluid (up to 7 ppm), the Li rich serpentine is likely to preserve its initial Li isotopic signature with little modification during this late-stage process. Thus Sr and Li may trace two distinct stages of the serpentinization process. However, the relict minerals have very low Li concentrations, so their Li compositions can be perturbed more easily than those of most serpentine. Thus the low δ^6Li values observed in the relict minerals, as well as in some serpentine with low Li contents, may reflect the addition of seawater Li, as well as of late-stage evolved fluids, during the low temperature process documented by the Sr isotopes. Nevertheless, mass balance indicates that these relict phases will have little influence on the δ^6Li of the whole rocks. To sum up, Li isotopic variations in serpentine are more sensitive to the early, hydrothermal stages of the serpentinization process, while the Sr variations reflect the later, seawater-dominated stages.

[27] The $\delta^{18}O$ variations observed in our samples range between 1.6 and 5.8‰. As $\delta^{18}O$ variations of fluid are limited between 0 and 2‰, for seawater and vent fluid respectively [*Teagle et al.*, 1998], variations of water-rock ratio will have only limited influence on the oxygen isotopic composition. Thus the main reason for $\delta^{18}O$ variations in serpentine is change of the water/rock exchange temperature. Li isotopes and content are also sensitive to this temperature. The isotopic fractionation between fluid and mineral increases at decreasing temperature, and the amount of Li deposited from the fluid will be proportional to the intensity of the fluid cooling. However, it is difficult to trace this process in detail, as we do not know the temperature variations of the fluid throughout its circulation path. The temperatures calculated from whole rock $\delta^{18}O$ analyses represent only mean values of a multistage process. The Li isotopic variations in serpentine are sensitive to both fluid composition and temperature, while the O variations mainly reflect fluid-rock interaction temperature.

5.2. Heterogeneities at Mineral Scale

[28] The wide range in Li contents and δ^6Li values in serpentine indicates that all serpentine in a given sample and even in a given mineral is not in equilibrium. *Kimball et al.* [1985] showed that secondary minerals of serpentinized peridotites formed at varying temperatures and in the presence of compositionally evolving altering fluid. Hence it is likely that both variation of the isotopic fractionation factor between mineral and fluid [*Chan and Edmond*, 1988; *Chan et al.*, 1992] with temperature and variation of fluid composition may contribute to creating the wide range of δ^6Li values observed in the serpentine. As explained above, early serpentine formed in the presence of the least evolved fluid has higher δ^6Li values and Li contents than later serpentine. In addition, the most positive δ^6Li values may be explained by a relatively low temperature of serpentine formation, implying high serpentine/fluid isotopic fractionation. Conversely, serpentine with the lowest δ^6Li values represents highly evolved fluids. Examination of Figure 6 indicates that,

as expected, very high and low δ^6Li values are rare compared to intermediate values. Concerning the relict minerals, their very low Li concentrations suggest that they lost much of their Li by leaching during hydrothermal circulation. These very low Li concentrations make the Li isotopic compositions of the relict phases susceptible to perturbation by interaction with late stage fluids and/or seawater, which have low Li contents and δ^6Li values.

[29] Changing conditions and patterns of fluid flow cause several generations of serpentine to be superimposed within each sample. This suggestion is plausible since circulation of fluid at low temperature is known to be irregularly distributed in the oceanic crust at slow spreading ridges [*Lécuyer and Fourcade*, 1991]. Consequently, we are dealing with an open system in which the conditions of alteration and the fluid chemistry are constantly changing. The heterogeneity observed within each sample indicates that the equilibration between fluid and serpentine is incomplete and that the bulk rock has not reequilibrated with the last fluid.

6. Conclusion

[30] The Li content and Li isotopic values of serpentinized peridotites from the southwest Indian Ridge strongly suggest that the Li composition of the hydrothermal fluid changes during serpentinization. Measured whole rock δ^6Li values ranging between −2.9 and −14‰ can be explained if Li in serpentinizing fluid is derived primarily from the ocean crust. This is not surprising, as seawater has a very low Li concentration that is easily overwhelmed by Li leached from the basalt as the fluid is heated during circulation. As serpentine forms, it incorporates Li and preferentially ^{6}Li, leaving fluid less rich in Li and with lower δ^6Li values. The evolution of the fluid composition combined with the changing conditions and patterns of fluid flow result in the superposition of several generations of serpentine. This results in considerable heterogeneity of both Li contents and Li isotopic compositions of serpentinized peridotites, occurring over both large and very small (<1 mm) length scales.

[31] The results presented here indicate that during serpentinization, Li transfer occurs mainly from fresh to altered ocean crust with only a minor contribution from seawater Li, which suggests that the effect of serpentinization on the seawater Li budget is minor. Therefore serpentinization cannot explain the apparent imbalance in this budget [*Stoffyn-Egli and Mackenzie*, 1984].

[32] Our results also demonstrate that the Li signature is dominated by the early stages of serpentinization, when the fluid is rich in Li, while Sr may reflect a later, superimposed process and O provides an indication of the average serpentinization temperature. Thus different isotopic systems provide different information about the very complex serpentinization process.

Acknowledgments

[33] The serpentinized peridotites were collected during the EDUL Cruise (*Marion Dufresne*, 1997) headed by C. Mével. We thank R. Brooker for providing some standards, as well as for his suggestions. The mass spectrometry analyses reported herein were made possible by the support of the E.U. Geochemical Facility at Bristol and access to the TIMS facility for R. James. We are grateful for the thoughtful comments of B. White, C. Chauvel, J. Ryan, H. Staudigel, and an anonymous reviewer.

References

Agrinier, P., and M. Cannat, Oxygen-isotope constraints on serpentinization processes in ultramafic rocks from the mid-atlantic ridge (23EN), in *Proc. Ocean Drill. Program, Sci. Results*, *153*, 381–388, 1997.

Agrinier, P., C. Mével, and J. Girardeau, Hydrothermal alteration of the peridotites cored at the ocean/continent boundary of the Iberian margin: petrologic and stable isotope evidence, in *Proc. Ocean Drill. Program, Sci. Results*, *103*, 225–233, 1988.

Anselmi, B., M. Mellini, and C. Viti, Chlorine in the Elba, Monti Livornesi and Murlo serpentines: Evidence for seawater interaction, *Eur. J. Mineral.*, *12*, 137–146, 2000.

Berger, G., J. Schott, and C. Guy, Behaviour of Li, Rb and Cs during basalt glass and olivine dissolution and chlorite, smectite and zeolite precipitation from seawater: Experimental investigations and modelization between 50° and 300°C, *Chem. Geol.*, *71*, 297–312, 1988.

Bonatti, E., J. R. Lawrence, and N. Morandi, Serpentinization of oceanic peridotites: temperature dependence of mineralogy and boron content, *Earth Planet. Sci. Lett.*, *70*, 88–94, 1984.

Brooker, R. A., R. H. James, and J. D. Blundy, Subduction-related mantle pyroxenites at Zabargad Island, Red Sea: Evidence from Li isotopes and trace element geochemistry, in *10th Annual V.M. Goldschmidt Conference, Oxford, J. Conf. Abstr* 5, *249*, 2000.

Chan, L. H., and J. M. Edmond, Variation of lithium isotope composition in the marine environment: a preliminary report, *Geochim. Cosmochim. Acta*, *52*, 1711–1717, 1988.

Chan, L. H., J. M. Edmond, G. Thompson, and K. Gillis, Lithium isotopic composition of submarine basalts: Implications for the lithium cycle in the ocean, *Earth Planet. Sci. Lett.*, *108*, 151–160, 1992.

Chan, L. H., J. M. Edmond, and G. Thompson, A lithium isotope study of hot springs and metabasalts from mid-ocean ridge hydrothermal systems, *J. Geophys. Res.*, *98*, 9653–9659, 1993.

Chan, L. H., L. Zhang, and J. R. Hein, Lithium isotope characteristics of marine sediments, *Eos Trans. AGU*, *75*, 314, 1994.

Chaussidon, M., F. Robert, D. Mangin, P. Hanon, and E. Rose, Analytical procedures for the measurement of boron isotope compositions by ion microprobe in meteorites and mantle rocks, *Geostand. News. J. Geostand. Geoanal.*, *21*, 7–17, 1997.

Coulton, A. J., G. D. Harper, and D. S. O'Hanley, Oceanic versus emplacement age serpentinization in the Josephine ophiolite: Implications for the nature of the Moho at intermediate and slow spreading ridges, *J. Geophys. Res.*, *100*, 22,245–22,260, 1995.

Deloule, E., C. France-Lanord, and F. Albarède, D/H analysis of minerals by ion probe, in *Stable Isotope Geochemistry: A Tribute to Samuel Epstein, Geochem. Soc. Spec. Publ.*, vol. 3, edited by H. P. Taylor, J. R. O'Neil and I. R. Kaplan, pp. 53–62, Geochem. Soc., San Antonio, Tex., 1991.

Deloule, E., M. Chaussidon, and P. Allé, Instrumental limitations for isotope measurements with a Cameca ims-3f ion microprobe: Example of H, B, S and Sr, *Chem. Geol.*, *101*, 187–192, 1992.

DeMets, C., R. G. Gordon, D. F. Argus, and C. Stein, Current plate motion, *Geophys. J. Int.*, *101*, 425–478, 1990.

Edmond, J. M., C. Measures, R. E. McDuff, L. H. Chan, R. Collier, and B. Grant, Ridge crest hydrothermal activity and the balances of the major and minor elements in the ocean: The Galapagos data, *Earth Planet. Sci. Lett.*, *46*, 1–18, 1979.

Flesch, G. D., A. R. Anderson Jr., and H. J. Svec, A secondary isotopic standard for $^{6}Li/^{7}Li$ determinations, *Int. J. Mass Spectrom. Ion Phys.*, *12*, 265–272, 1973.

Früh-Green, G. L., A. Plas, and C. Lécuyer, Petrologic and stable isotope constraints on hydrothermal alteration and serpentinization of the EPR shallow mantle at Hess Deep (Site 895), *Proc. Ocean Drill. Program, Sci. Results*, *147*, 255–291, 1996.

Huh, Y., L. H. Chan, L. Zhang, and J. M. Edmond, Lithium and its isotopes in major world rivers: Implications for weathering and the oceanic budget, *Geochim. Cosmochim. Acta*, *62*, 2039–2051, 1998.

James, R. J., and M. R. Palmer, The lithium isotope composition of international rock standards and solutions, *Chem. Geol.*, *166*, 319–326, 2000.

James, R. J., H. Elderfield, and M. R. Palmer, The chemistry of hydrothermal fluids from Broken Spur site, 29°N Mid - Atlantic Ridge, *Geochim. Cosmochim. Acta*, *59*, 651–659, 1995.

Kimball, K. L., and D. Gerlach, Sr isotopic constraints on hydrothermal alteration of ultramafic rocks in two oceanic fracture zones from the South Atlantic Ocean, *Earth Planet. Sci. Lett.*, *78*, 177–188, 1986.

Kimball, K. L., F. S. Spear, and H. J. B. Dick, High temperature alteration of abyssal ultramafics from the Islas Orcadas fracture zone, South Atlantic, *Contrib. Mineral. Petrol.*, *91*, 307–320, 1985.

Lécuyer, C., and S. Fourcade, Oxygen isotope evidence for multi-stage hydrothermal alteration at a fossil slow-spreading center: The Silurian Trinity ophiolite (California, U.S.A.), *Chem. Geol.*, *87*, 231–246, 1991.

Macdonald, A. H., and W. S. Fyfe, Rate of serpentinization in seafloor environments, *Tectonophysics*, *116*, 123–135, 1985.

McCollom, T. M., and E. Shock, Fluid-rock interactions in the lower oceanic crust: thermodynamic models of hydrothermal alteration, *J. Geophys. Res.*, *103*, 547–575, 1998.

Mével, C., et al., *Report EDUL Cruise MD107 N/O Marion Dufresne*, 184 pp., Lab. Pétrologie, Univ. P.M. Curie, Paris, France, 1997.

Morozov, N. P., Geochemistry of rare alkaline elements in the oceans and seas, *Oceanology*, *8*, 169–178, 1968.

Prichard, H. M., A petrographic study of the processes of serpentinization in ophiolites and the ocean crust, *Contrib. Mineral. Petrol.*, *68*, 231–241, 1979.

Rucklidge, J. C., Chlorine in partially serpentinized dunite, *Econ. Geol.*, *67*, 38–40, 1972.

Ryan, J. G., and C. H. Langmuir, The systematics of lithium abundances in young volcanic rocks, *Geochim. Cosmochim. Acta*, *51*, 1727–1741, 1987.

Seitz, H.-M., and A. B. Woodland, The distribution of lithium in peridotitic and pyroxenitic mantle lithologies — An indicator of magmatic and metasomatic processes, *Chem. Geol.*, *166*, 47–64, 2000.

Seyfried, W. E., D. R. Janecky, and M. J. Mottl, Alteration of the oceanic crust: implications for geochemical cycles of lithium and boron, *Geochim. Cosmochim. Acta*, *48*, 557–569, 1984.

Steuber, A. M., W. H. Huang, and W. D. Johns, Chlorine and fluorine in ultramafic rocks, *Geochim. Cosmochim. Acta*, *32*, 353–358, 1968.

Stoffyn-Egli, P., and F. T. Mackenzie, Mass balance of dissolved lithium in the oceans, *Geochim. Cosmochim. Acta*, *48*, 859–872, 1984.

Teagle, D. A. H., J. C. Alt, H. Chiba, S. E. Humphris, and A. N. Halliday, Strontium and oxygen isotopic constraints on

fluid mixing, alteration and mineralization in the TAG hydrothermal deposit, *Chem. Geol.*, *149*, 1–24, 1998.

Von Damm, K. L., B. Grant, and J. M. Edmond, Preliminary report on the chemistry of hydrothermal solutions at 21°N, East Pacific Rise, in *Hydrothermal Processes at Seafloor Spreading Centers*, edited by P. A. Rona, K. Boström, L. Laubier, and K. L. S. Smith, p. 369, Plenum, New York, 1983.

Wenner, D. B., and H. P. Taylor, Temperatures of serpentinization of ultramafic rocks based on $^{18}O/^{16}O$ fractionation between coexisting serpentine and magnetite, *Contrib. Mineral. Petrol.*, *32*, 165–185, 1971.

Wicks, F. J., and E. J. W. Whittaker, Serpentine textures and serpentinization, *Can. Mineral.*, *15*, 459–488, 1977.

You, C. F., L. H. Chan, A. J. Spivack, and J. M. Gieskes, Lithium, boron, and their isotopes in sediments and pore waters of ocean drilling program Site 808, Nankai Trough: Implications for fluid expulsion in accretionary prisms, *Geology*, *23*, 37–40, 1995.

Zhang, L., L. H. Chan, and J. M. Gieskes, Lithium isotope geochemistry of pore waters from Ocean Drilling Program Sites 918 and 919, Irminger Basin, *Geochim. Cosmochim. Acta*, *62*, 2437–2450, 1998.